

On the relationship between small and large signal modulation capabilities in highly nonlinear quantum dot lasers

Original

On the relationship between small and large signal modulation capabilities in highly nonlinear quantum dot lasers / D., Gready; G., Eisenstein; Giannini, Mariangela; Montrosset, Ivo; D., Arsenijevic; H., Schmeckebier; M., Stubenrauch; D., Bimberg. - In: APPLIED PHYSICS LETTERS. - ISSN 0003-6951. - STAMPA. - 102:10(2013), pp. 101107 -1-101107 -3. [10.1063/1.4795130]

Availability:

This version is available at: 11583/2519725 since:

Publisher:

AIP American Institute of Physics

Published

DOI:10.1063/1.4795130

Terms of use:

This article is made available under terms and conditions as specified in the corresponding bibliographic description in the repository

Publisher copyright

(Article begins on next page)



On the relationship between small and large signal modulation capabilities in highly nonlinear quantum dot lasers

D. Gready, G. Eisenstein, M. Gioannini, I. Montrosset, D. Arsenijevic, H. Schmeckebier, M. Stubenrauch, and D. Bimberg

Citation: *Applied Physics Letters* **102**, 101107 (2013); doi: 10.1063/1.4795130

View online: <http://dx.doi.org/10.1063/1.4795130>

View Table of Contents: <http://scitation.aip.org/content/aip/journal/apl/102/10?ver=pdfcov>

Published by the [AIP Publishing](#)

An advertisement for Integrated Engineering Software. On the left is a logo consisting of a purple square with a white dot pattern. To its right, the text 'INTEGRATED ENGINEERING SOFTWARE' is written in a bold, dark blue, sans-serif font. Below this, the text 'Particle and Beam Ray Tracing Simulation' is in a dark grey font, followed by 'Send us your model and see LORENTZ in action' in a lighter grey font. At the bottom right of the text area, the words 'LEARN MORE' are written in a white, bold, sans-serif font, slanted upwards. On the right side of the advertisement is a 3D visualization of a particle beam simulation, showing a cross-section of a beam with various colored regions (blue, green, red) and a central red beam path. The background is a light yellow with faint white dotted lines.

On the relationship between small and large signal modulation capabilities in highly nonlinear quantum dot lasers

D. Gready,^{1,a)} G. Eisenstein,¹ M. Giovannini,² I. Montrosset,² D. Arsenijevic,³ H. Schmeckeber,³ M. Stubenrauch,³ and D. Bimberg³

¹Electrical Engineering Department, Technion, Haifa 32000, Israel

²Department of Electronics and Telecommunications, Politecnico di Torino, Torino 10129, Italy

³Institute of Solid-State Physics, Technische Universität Berlin, Berlin, Germany

(Received 7 January 2013; accepted 27 February 2013; published online 13 March 2013)

The small signal modulation response of semiconductor lasers is commonly used to predict large signal modulation capabilities. Recent experiments suggest that this prediction may fail in some quantum dot (QD) lasers. We present a model supported by experiments, which shows that when the small signal modulation response is limited by gain compression and the gain is large, the laser can be modulated at very high bit rates. This effect is inherent to dynamics governing all semiconductor lasers but the conditions needed for high bit rate modulation in the presence of narrow small signal bandwidths are only obtainable in QD lasers. © 2013 American Institute of Physics. [<http://dx.doi.org/10.1063/1.4795130>]

The small signal bandwidth of semiconductor lasers is commonly used as a predictor to their large signal modulation capabilities. A given bandwidth of F GHz is assumed to enable modulation at $\sim F/0.7$ Gbit/s,¹ similar to the case of linear and quasi linear systems such as modulators and receivers. Dynamical properties of quantum dot (QD) lasers have been studied for many years² and basic modulation properties are well documented. Recent reported experiments^{3,4} showed, however, that in some QD lasers, the small signal bandwidth may vastly underestimate the digital modulation capabilities. In Ref. 3, a GaAs laser emitting at $1.3 \mu\text{m}$ with a bandwidth of 11 GHz was modulated at 25 Gbit/s. This laser comprised eight dot layers and had a modal gain of 46 cm^{-1} . In Ref. 4, an InP based QD laser, where four dot layers were used yielding a modal gain of 40 cm^{-1} showed a bandwidth of 5 GHz and was modulated successfully at 15 Gbit/s. These results were attributed⁵ to the complexity of carrier and gain dynamics in QD lasers.

It is well known that the small signal bandwidth in most QD lasers is limited by the large nonlinear gain compression factor (commonly known as ε)^{5–7} and by the moderate modal gain.^{8,9} Recent advances in QD material growth led to impressive increases in the gain^{10,11} but since ε remains large, the small signal bandwidth in all reported QD lasers does not exceed 10–12 GHz, except for QD lasers exploiting tunneling injection at $\sim 1 \mu\text{m}$.¹² It turns out that the two reported QD lasers exhibiting digital modulation at large bit rates^{3,4} have particularly large modal gain values. We postulated, therefore, that large gain lasers whose small signal is limited by a large ε (which may stem from basic material nonlinearity or from long transport times¹³) may be modulated at large bit rates. We demonstrate our hypothesis using a standard model for QD laser dynamics, which we compare with a new experiment describing the modulation properties of a GaAs QD laser emitting near $1.3 \mu\text{m}$. We further show that the dynamical properties we explore are inherent to the nature of the carrier and gain dynamics of all semiconductor lasers.

However, the conditions of an ε , which is sufficiently large to limit the small signal bandwidth and a large gain, are only obtainable in practice in QD lasers.

In order to motivate the modeling, we present experimental characterizations of a QD laser comprising 15 layers of InGaAs QDs with a nominal thickness of 2.5 monolayers separated by 33 nm GaAs barriers. The large number of QD layers and the very wide barriers are responsible for major carrier transport limitations, which yield a very large ε . Indeed, the measured small signal modulation response shown in Fig. 1(a) reveals a highly damped response with a very narrow bandwidth of only 2 GHz. The modal gain of a similar laser was measured in Ref. 8 to be $\sim 3.6 \text{ cm}^{-1}$ per QD layer; the large total gain results of course from the large number, 15, of QD layers. The large signal modulation properties were examined using a pseudo random bit streams at various rates, bias levels, and drive current amplitudes. The best result is presented in Fig. 1(b), which shows a clearly open eye diagram at 8.5 Gbit/s with an on/off ratio of 3 dB. This modulation rate is not possible by simple predictions based on Fig. 1(a). However, we show below that both the small and large signal modulation capabilities are consistent with modeling provided that the proper device and material parameters and operation conditions are used.

The QD laser was modeled using a standard four energy levels rate equation model similar to Ref. 14 with only one carrier type (electrons) injected in a cascaded process and two photon density rate equations describing emission from the excited and ground states. The carrier injection scheme is depicted in Fig. 2. Carriers are injected into the separate confinement heterostructure (SCH) and relax into the QD ground state via the wetting layer (WL) and QD excited state. The model is formulated in Eqs. (1)–(6). Common parameter values were used in the simulation.¹⁴ Specifically, a large value of $\varepsilon = 2.0475 \times 10^{-6}$ was chosen to accommodate the highly damped measured small signal modulation response shown in Fig. 1(a). The parameter ε is given here in a somewhat unconventional manner as it is normalized to the gain region volume. It corresponds to $\varepsilon = 10^{-15} \text{ cm}^3$ in the regular

^{a)}davidgr@tx.technion.ac.il.

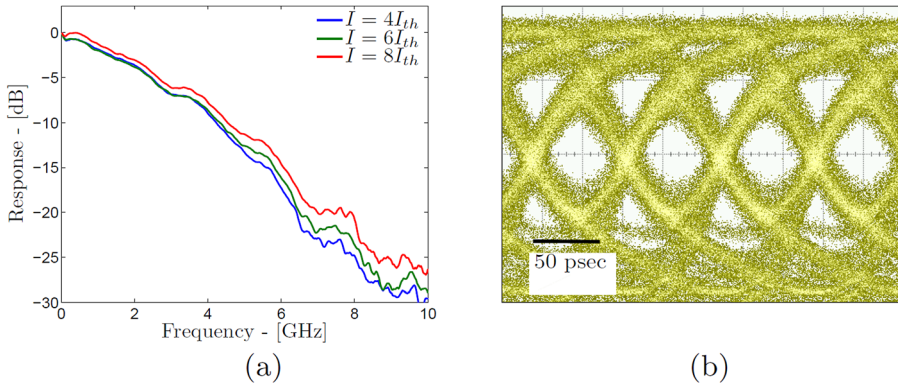


FIG. 1. (a) Small signal modulation response of a 1.3 μm QD laser. (b) Eye diagram of a 1.3 μm QD laser at 8.5 Gbit/s. These responses are the ones modeled in the paper with calculated results shown in Figs. 3(a) and 3(b).

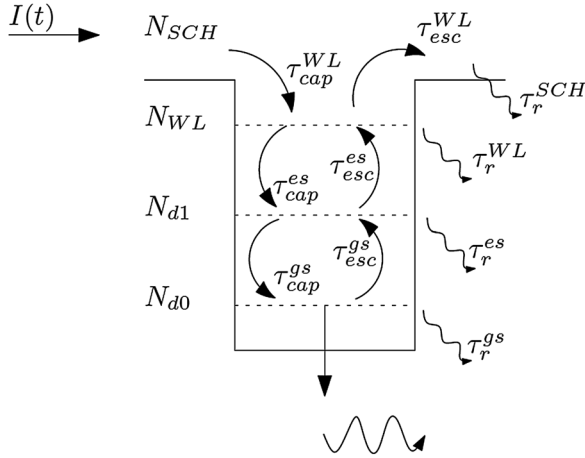


FIG. 2. A schematic description of the injection path of a QD laser.

formalism. The laser gain was chosen according to Ref. 8 to be $g = 3.6 \text{ cm}^{-1}$ per QD layer. Other key parameters are the QD areal density and capture time constants, which were chosen to be $N_D = 3 \times 10^{10} \text{ cm}^{-2}$, $\tau_{\text{cap}}^{\text{WL}} = 1 \text{ ps}$, $\tau_{\text{cap}}^{\text{es}} = 10 \text{ ps}$, and $\tau_{\text{cap}}^{\text{gs}} = 150 \text{ fs}$. Escape time constants are set according to a quasi-equilibrium distribution. A solution of the model results in the small signal response shown in Fig. 3(a) and the large signal modulation (at 8.5 Gbit/s) shown in Fig. 3(b). Both fit well to the measurements. Calculations using the same ε but a lower gain yield a very similar small signal response but a completely closed eye at any bit rate above 5 Gbit/s. As a second example, we simulated the response of the laser presented in Ref. 3 using the QD laser model described in Ref. 15. Once more, due to the large gain and nonlinear gain compression factor, a small signal bandwidth of 11 GHz and large signal modulation at 20 Gbit/s and 25 Gbit/s were

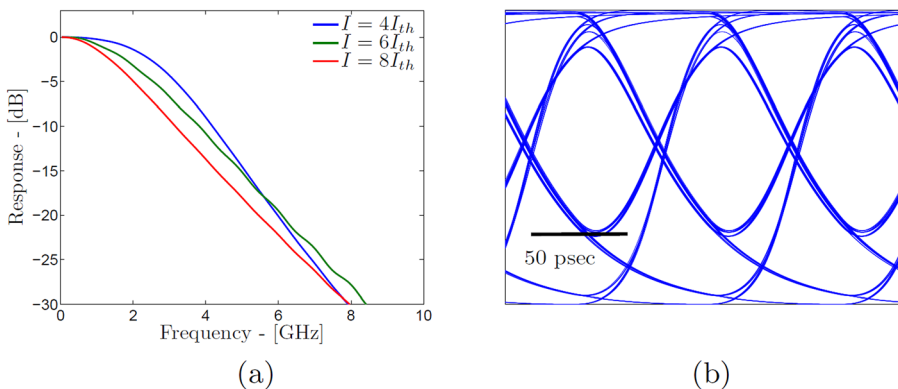


FIG. 3. (a) Simulated small signal modulation response of a 1.3 μm QD laser. (b) Simulated eye diagram of a 1.3 μm QD laser at 8.5 Gbit/s. The simulations confirm the experimental results shown in Figs. 1(a) and 1(b).

found in the simulation fitting very well to the published experimental results. The simulations suggest a very high gain compression factor, which is often found in QD lasers.⁶

$$\frac{dN_{SCH}}{dt} = \frac{I(t)}{q} - \frac{N_{SCH}}{\tau_{\text{cap}}^{\text{WL}}} - \frac{N_{SCH}}{\tau_r^{\text{SCH}}} + \frac{N_{WL}}{\tau_{\text{esc}}^{\text{WL}}}, \quad (1)$$

$$\frac{dN_{WL}}{dt} = \frac{N_{SCH}}{\tau_{\text{cap}}^{\text{WL}}} + \frac{N_{es}}{\tau_{\text{esc}}^{\text{es}}} - \frac{N_{WL}}{\tau_{\text{esc}}^{\text{WL}}} - \frac{N_{WL}}{\tau_r^{\text{WL}}} - \frac{N_{WL}}{\tau_{\text{cap}}^{\text{es}}} \left(1 - \frac{N_{es}}{4N_d}\right), \quad (2)$$

$$\begin{aligned} \frac{dN_{es}}{dt} = & \frac{N_{WL}}{\tau_{\text{cap}}^{\text{es}}} \left(1 - \frac{N_{es}}{4N_d}\right) + \frac{N_{gs}}{\tau_{\text{esc}}^{\text{gs}}} \left(1 - \frac{N_{es}}{4N_d}\right) - \frac{N_{es}}{\tau_r^{\text{es}}} - \frac{N_{es}}{\tau_{\text{esc}}^{\text{es}}} \\ & - \frac{N_{es}}{\tau_{\text{cap}}^{\text{gs}}} \left(1 - \frac{N_{gs}}{2N_d}\right) - \Gamma \frac{c \cdot g_{es}}{n} \left(\frac{N_{es}}{2N_d} - 1\right), \end{aligned} \quad (3)$$

$$\begin{aligned} \frac{dN_{gs}}{dt} = & \frac{N_{es}}{\tau_{\text{cap}}^{\text{gs}}} \left(1 - \frac{N_{gs}}{2N_d}\right) - \frac{N_{gs}}{\tau_{\text{esc}}^{\text{gs}}} \left(1 - \frac{N_{es}}{4N_d}\right) - \frac{N_{gs}}{\tau_r^{\text{gs}}} \\ & - \Gamma \frac{c \cdot g_{gs}}{n} \left(\frac{N_{gs}}{N_d} - 1\right), \end{aligned} \quad (4)$$

$$\frac{dS_{es}}{dt} = \Gamma \frac{c \cdot g_{es}}{n} \left(\frac{N_{es}}{2N_d} - 1\right) \cdot S_{es} \cdot \frac{1}{1 + \varepsilon \cdot S} - \frac{S_{es}}{\tau_{\text{ph}}^{\text{es}}} + \beta_{es} \cdot \frac{N_{es}}{\tau_r^{\text{es}}}, \quad (5)$$

$$\frac{dS_{gs}}{dt} = \Gamma \frac{c \cdot g_{gs}}{n} \left(\frac{N_{gs}}{N_d} - 1\right) \cdot S_{gs} \cdot \frac{1}{1 + \varepsilon \cdot S} - \frac{S_{gs}}{\tau_{\text{ph}}^{\text{gs}}} + \beta_{gs} \cdot \frac{N_{gs}}{\tau_r^{\text{gs}}}. \quad (6)$$

To further understand the dynamical behavior of the QD laser, we analyze the small signal response in terms of its poles dependence on I/I_{th} . The results are shown in Fig. 4. The green line in Fig. 4 represents the complex conjugate low

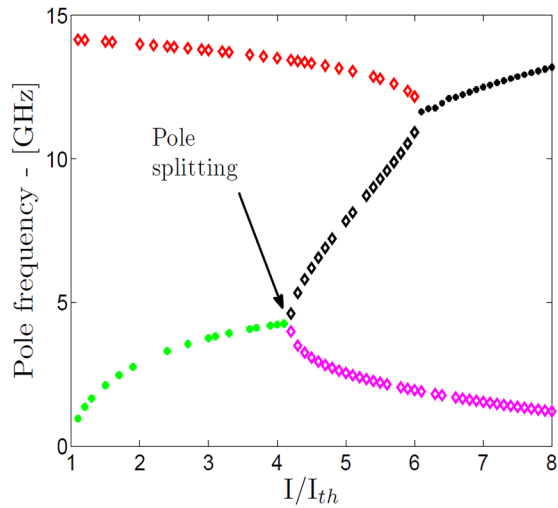


FIG. 4. Small signal modulation transfer function poles map versus injected current.

frequency poles that determine the modulation bandwidth. The red line represents real poles at higher frequency, whose origin is the capture of carriers from high energy states to the QD. At some bias level, the response changes so that it is characterized by two real poles one of which is at a high frequency (black diamond shaped marks in Fig. 4). Under such conditions, the small signal modulation response decreases beyond the electron-photon resonance at a slower rate than the common 40 dB per decade, just as in a highly damped response. The best large signal modulation response is obtained at a bias level near the poles splitting point. In principle, this pole splitting may occur in any laser. However, since it depends on saturation, it is reached in a QD laser for low values of I/I_{th} and is therefore easily achieved. This can be easily understood from a classical analysis,¹⁶ which calculates the photon number under the condition of maximum bandwidth Eq. (7) when the resonance frequency and the damping factor are related by $\omega_p = 0.707\gamma$.

$$S_{TP} = (N_{Tth} - N_{Tr}) / \{1 + V_p^2 \cdot (N_{Tth} - N_{Tr})^2 / \varepsilon^2\}, \quad (7)$$

where N_{Tth} and N_{Tr} are the number of carriers at threshold and transparency, respectively. V_p and ε are the photon volume and gain compression factor, respectively. In small dimensional gain media, the maximum photon density is easily reached due to the small density of carriers in the lasing states and due to the large value of gain compression factor. Finally, it is easy to show that a simple rate equation analysis of conventional bulk and QW lasers,¹⁷ in which both the gain and the nonlinear gain compression are chosen to be large, yields similar results. That is, a small signal response which is clearly limited by the nonlinear gain compression may avail large signal modulation at high bit rates. An example is shown in Fig. 5, which was calculated for a gain of 60 cm^{-1} and a nonlinear gain compression parameter $\varepsilon = 4 \times 10^{-6}$. Indeed, this calculated response exhibits a very damped behavior with a bandwidth of about 2 GHz, but large signal modulation at 8 Gbit/s with an on/off ratio of 3 dB is

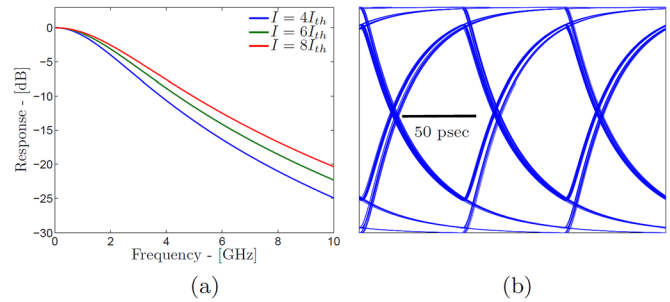


FIG. 5. (a) Simulated small signal modulation response of a bulk semiconductor laser. (b) Simulated eye diagram of a bulk semiconductor laser at 8 Gbit/s with 3 dB on/off ratio.

nevertheless possible. However, the parameters chosen can only be reached in practical QW lasers at extremely large values of I/I_{th} , which are not practical.

To conclude, we have analyzed the relationship between small and large signal modulation capabilities of semiconductor lasers. We have demonstrated experimentally that QD lasers with a high gain and a large nonlinear gain compression have narrow small signal bandwidths but are capable of large signal modulation at very high rates. The reason for this behavior is shown to be due to an inherent property of diode lasers. However, the conditions for which this property can manifest itself are only practical in low dimensional gain media such as QDs.

¹D. Derickson and C. Hentschel, *Fiber Optic Test and Measurement* (Prentice-Hall PTR, New Jersey, 1998).

²D. Bimberg, N. Kirstaedter, N. Ledentsov, Z. Alferov, P. Kop'ev, and V. Ustinov, *IEEE J. Sel. Top. Quantum Electron.* **3**, 196 (1997).

³M. Ishida, M. Matsuda, Y. Tanaka, K. Takada, M. Ekawa, T. Yamamoto, T. Kageyama, M. Yamaguchi, K. Nishi, M. Sugawara *et al.*, in *Conference on Lasers and Electro-Optics (CLEO) and Quantum Electronics and Laser Science Conference (QELS)* (2010), p. 1.

⁴D. Gready, G. Eisenstein, C. Gilfert, V. Ivanov, and J. P. Reithmaier, *IEEE Photonics Technol. Lett.* **24**, 809 (2012).

⁵A. Fiore and A. Markus, *IEEE J. Quantum Electron.* **43**, 287 (2007).

⁶F. Grillot, B. Dagens, J. Provost, H. Su, and L. Lester, *IEEE J. Quantum Electron.* **44**, 946 (2008).

⁷A. Capua, L. Rozenfeld, V. Mikhelashvili, G. Eisenstein, M. Kuntz, M. Laemmlin, and D. Bimberg, *Opt. Express* **15**, 5388 (2007).

⁸A. Kovsh, N. Maleev, A. Zhukov, S. Mikhlin, A. Vasilev, E. Semenova, Y. Shernyakov, M. Maximov, D. Livshits, V. Ustinov *et al.*, *J. Cryst. Growth* **251**, 729 (2003).

⁹H. Dery and G. Eisenstein, *IEEE J. Quantum Electron.* **41**, 26 (2005).

¹⁰C. Gilfert, V. Ivanov, N. Oehl, M. Jacob, and J. P. Reithmaier, *Appl. Phys. Lett.* **98**, 201102 (2011).

¹¹Y. Tanaka, M. Ishida, K. Takada, Y. Maeda, T. Akiyama, T. Yamamoto, H. Z. Song, M. Yamaguchi, Y. Nakata, K. Nishi, M. Sugawara, and Y. Arakawa, in *LEOS Annual Meeting Conference Proceeding* (2009), p. 668.

¹²P. Bhattacharya, S. Ghosh, S. Pradhan, J. Singh, Z. K. Wu, J. Urayama, K. Kim, and T. B. Norris, *IEEE J. Quantum Electron.* **39**, 952 (2003).

¹³N. Tessler, R. Nagar, and G. Eisenstein, *IEEE J. Quantum Electron.* **28**, 2242 (1992).

¹⁴M. Gioannini, A. Sevega, and I. Montrosset, *IEEE Opt. Quantum Electron.* **38**, 381 (2006).

¹⁵M. Gioannini and I. Montrosset, *IEEE J. Quantum Electron.* **43**, 941 (2007).

¹⁶L. A. Coldren and S. W. Corzine, *Diode Lasers and Photonic Integrated Circuits* (Wiley, 1995).

¹⁷R. Tucker and I. Kaminow, *J. Lightwave Technol.* **2**, 385 (1984).